Free-Fall Behavior of Planar Snow Crystals, Conical Graupel and Small Hail

ROLAND LIST AND ROBERT S. SCHEMENAUER

Dept. of Physics, University of Toronto, Toronto, Canada

(Manuscript received 7 July 1970)

ABSTRACT

Drag coefficients and Best numbers of models of six planar snow crystals, two conical graupel and two conical small-hail particles were determined experimentally in glycerin-water mixtures and salt solutions. The Reynolds number (Re) range covered for the crystals was 0.1 to 200 and for the conical models 10 to 2000. It was found that the drag coefficients of dendritic shapes differed by factors of up to 4 from that of a disc of equal thickness and at an equal Reynolds number. The drag ratio is roughly constant with Re and linearly related to the ratio of the respective surface areas. The drag coefficients of the conical models assumed values between 0.5 and 2.0. During steady fall they decreased with increasing Re; however, as soon as oscillations started this trend reversed. Since tumbling does occur for larger graupel and small hail at Re>300–1000 their main characteristic motions and frequencies are also discussed. Values for oscillation frequencies are given and the motions are described in detail.

1. Introduction

A knowledge of drag coefficients and characteristic motions such as translations, oscillations and rotations of snow crystals, graupel and small hail in free fall is necessary for the understanding of their formation in nature, and, as a result, for the growth of hail or rain by the Bergeron-Findeisen process.

Measurements of the sizes and/or the fall velocities of different shapes of *snow crystals* by various authors indicate that the range of Reynolds number in the atmosphere is $1<\mathrm{Re}<200$ [see, for example, Nakaya and Terada (1934)]. In the literature, the least satisfactory data are to be found for planar snow crystals. This may have led Podzimek (1965) to perform a series of water tank experiments with models of snow crystals, their characteristic movements being briefly described for $10<\mathrm{Re}<19{,}000$. Podzimek (1968), based on the same data, gave the drag coefficient of hexagonal plates for $\mathrm{Re}<200$ as $C_D=16.5\ \mathrm{Re}^{-0.466}$ [confirmed by Jayaweera and Cottis (1969)] and of stars with narrow or broad arms and plates with outgrows as $C_D=20.2\ \mathrm{Re}^{-0.466}$. This latter formula, however, does not distinguish between the different shapes.

Measurements on *graupel* and *small hail* suggest Reynolds numbers in the range $10<\mathrm{Re}<2000$, with the majority probably between 100 and 1000. Some aspects of the motions of conical models were discussed by Nagel (1962), Jayaweera and Mason (1965), Goldburg and Florsheim (1966) and others; however, proper drag coefficients for the right shapes and in the required Reynolds number range are still lacking.

The purpose of this investigation, therefore, is to fill this gap by studying the free-fall behavior of stellar snow crystals, conical graupel and small hail.

2. Methods and apparatus

The terminal speed of precipitation particles can be calculated if the drag coefficient C_D is known as a function of the Reynolds number. The drag coefficient is defined by

$$C_D=\frac{2gQ\Delta\rho}{\rho_f V^2 S}, \tag{1}$$

where g is the acceleration due to gravity, Q the volume of the particle, $\Delta\rho$ the difference of the particle and fluid densities, ρ_f the fluid density, V its terminal speed, and S the cross-sectional area of the particle presented to the flow.

When C_D is not merely a constant but a function of the Reynolds number ($\mathrm{Re}=VD\rho_f\eta^{-1}$, with D the characteristic length and η the dynamic viscosity), and the condition of free fall provides a relationship between terminal speed and characteristic length, then it is advantageous to define a new dimensionless number, the Best number Be, i.e.,

$$\mathrm{Be}=\left(\frac{2Q\Delta\rho D^2}{S}\right)\left(\frac{g\rho_f}{\eta^2}\right)=C_D\mathrm{Re}^2. \tag{2}$$

The Best number, established by Best (1950), depends only on particle characteristics and atmospheric parameters, but not on speed and drag.

The experiments to determine drag and Best numbers as functions of Re consisted of a simulation of the free fall of particles in air by free fall in glycerin-water mixtures and salt solutions. Such a procedure is perfectly adequate as long as the Navier-Stokes equation necessary for the description of such situations does not

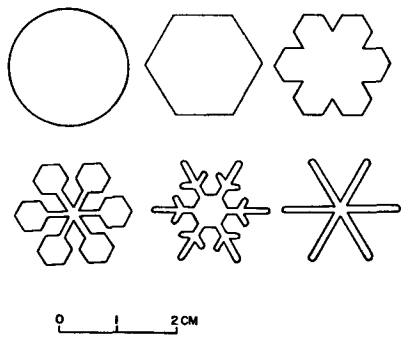

FIG. 1. Snow crystal models: top row, left to right—disc, hexagonal plate and broad-branched crystal; bottom row, left to right—stellar crystal with plates, dendrite and stellar crystal.

contain a local time derivative (List, 1966). Then the Reynolds number is the sole independent dimensionless number to characterize the flow. However, as soon as the particles do not fall steadily, but oscillate, rotate or move horizontally, then Strouhal numbers (giving characteristic frequencies or even frequency spectra) have to be considered. Due to the fact that these secondary motions were either non-existent or rather small in a majority of the experiments described below, this effect of non-steadiness on simulation is assumed to be negligible for the time being.

Two sets of six snow crystal models were made, one from polished duralumin and one from polished brass. The shapes chosen were typical of plane crystals: a hexagonal plate, a broad-branched crystal, a stellar crystal with plates, a dendrite, a stellar crystal, and a disc for reference. The cross-sectional areas of the models (shown in Fig. 1) are, respectively: 2.62, 2.31, 1.48, 0.87, 0.57 and 3.14 cm^2. All models were cut from a disc of diameter 2.0 cm and thickness 0.08 cm. The thicknesses of the models were not varied since Jayaweera and Cottis (1969) found the drag coefficients of discs to be independent of the thickness-to-diameter ratio for $0.2<\mathrm{Re}<100$ if this ratio varied between 0.01 and 0.8.

A set of four conical models, with spherical segments for bases, two representing conical graupel and two representing small hail particles were machined from perspex and polished. Three of the cones had apex angles of 90° and the fourth 70° (Fig. 2 and Table 1), similar to the models used by List (1959) and in agreement with natural shapes (List, 1958). No attempt was made to incorporate roughness elements.

The measurements were made in two perspex tanks, the larger having dimensions of $49\times51\times100$ cm and the smaller $25\times25\times50$ cm. Both tanks were equipped with

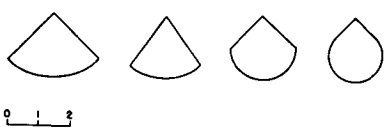

FIG. 2. Conical models: left to right—90° cone-spherical sector, 70° cone-spherical sector, 90° cone-hemisphere and 90° teardrop.

TABLE 1. Dimensions of conical models.

Model type	Apex angle α	Cone base diameter D (cm)	Total height H (cm)	Volume Q (cm^3)
90° cone-spherical segment	90°	2.90	2.07	5.542
70° cone-spherical segment	70°	2.28	1.98	3.172
90° cone-hemisphere	90°	1.99	1.94	3.054
90° teardrop	90°	1.61	1.87	2.209

catching screens which could be raised or lowered for retrieving the models. The large tank was used with salt solutions, the small with mixtures of glycerin and water. Densities were determined with a set of precision hydrometers, and the viscosity was measured with a calibrated Ostwald viscometer. Approximately 1400 stopwatch measurements were made of the fall times of the models between two levels in the tanks, yielding values of drag coefficients at various Reynolds numbers. The two sets of results, taken in the two tanks, blended together in the overlapping Re range without any discontinuity. The models were photographed stroboscopically with a 35-mm still camera as they fell, and 8- and 16-mm movie cameras were frequently used. This allowed measurement of oscillation frequencies as well as wavelengths and amplitudes of any model motions.

3. Results

The drag coefficients and Best numbers of the six snow crystal models are shown in Fig. 3 as functions of Reynolds number (which is based on a characteristic length equivalent to the model diameter). The Best numbers of the models follow directly from the drag coefficient results using $\mathrm{Be}=C_D\mathrm{Re}^2$. The curves are approximately parallel and show a decrease in drag coefficient as the Reynolds number is increased. It is often assumed that the aerodynamics of planar snow crystals can be approximated by data obtained from freely falling discs. From Fig. 3 we see that over the range $0.1<\mathrm{Re}<100$, the drag coefficient of a hexagonal plate is on the average 14% higher than that of a disc at the same Reynolds number. *Dendritic crystal models have drag coefficients up to four times that of a disc.* Data for discs are thus seen to be applicable to other planar crystals only to an order of magnitude approximation.

For the six planar snow crystal models tested, no oscillations were observed for $\mathrm{Re}\leqslant100$. By $\mathrm{Re}\approx200$ small oscillations were only observed in the disc, hexagonal plate and broad-branched crystal models, the oscillations being the greatest in the case of the disc.

As the cross-sectional area S of the models decreased, the drag coefficient increased for a given Reynolds number. This is not unexpected since the decrease in S coincides in general with an increase in the perimeter of the crystal.

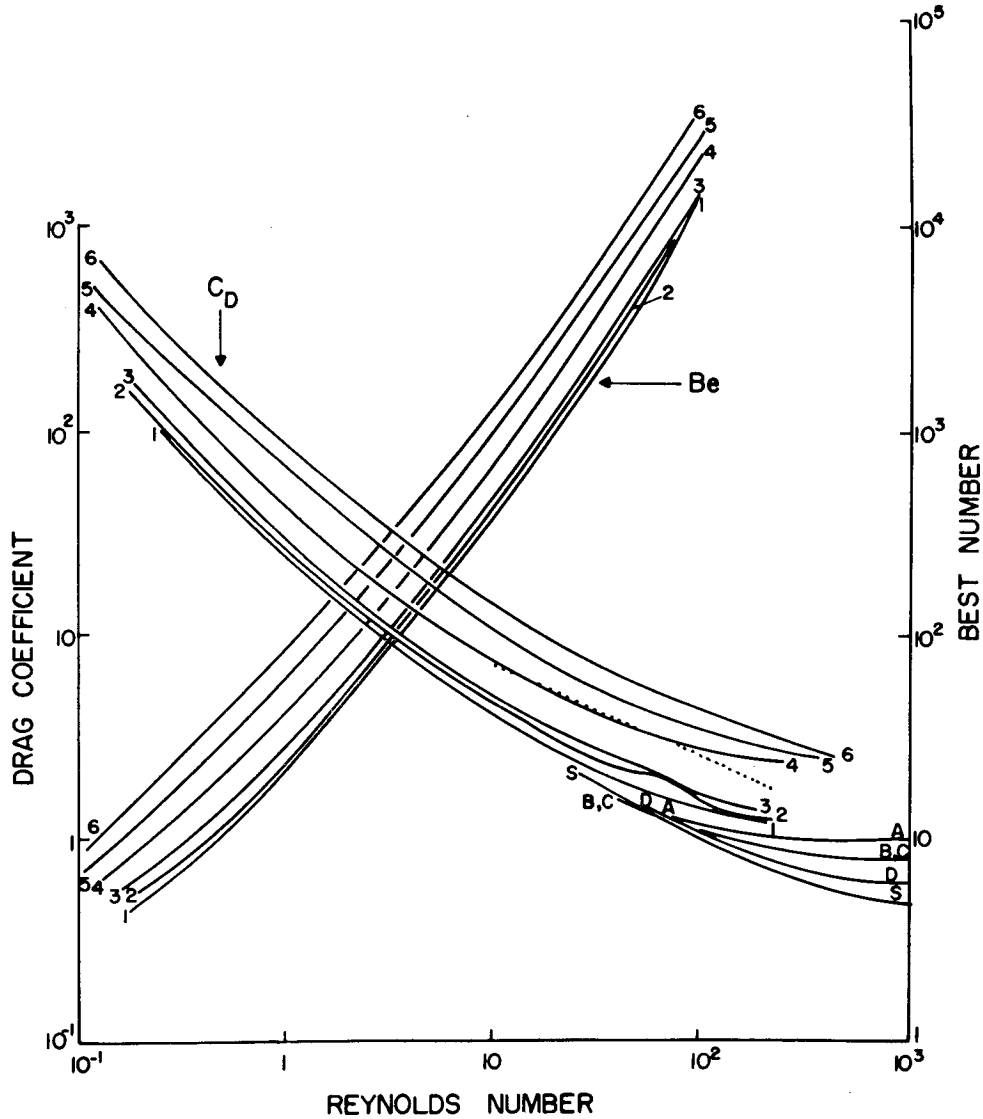

FIG. 3. Drag coefficients and Best numbers of snow crystal models as functions of Reynolds number: 1 disc, 2 hexagonal plate, 3 broad-branched crystal, 4 stellar crystal with plates, 5 dendrite, 6 stellar crystal; A 90° cone-spherical sector, B 70° cone-spherical sector, C 90° cone-hemisphere, D 90° teardrop, S sphere. The drag coefficients for the sphere are from Wieselsberger (1922). The dotted line representing stars with narrow or broad arms and plates with outgrows is from Podzimek (1968).

In Fig. 4 the ratio of the drag coefficients for the six model crystals to that for the disc is plotted as a function of the ratio of the corresponding cross-sectional areas. Although the ratio of the cross-sectional areas was chosen as the descriptive parameter, it is the same as the volume or mass ratio, since the densities and thicknesses of the models are identical. A least-squares technique was used to determine the best fitting straight line. Based on measurements in the range $1.2<S_{\text{disc}}/S_{\text{crystal}}<5.5$, the drag coefficient of a plane crystal can be determined from

$$C_{D\text{crystal}}=C_{D\text{disc}}(0.53+0.56S_{\text{disc}}/S_{\text{crystal}}). \quad (3)$$

The measurements of the drag coefficient of discs agreed very well with those of Willmarth *et al.* (1964) and Jayaweera and Mason (1965).

The drag coefficients and Best numbers of the four conical models, released in the apex down position, are shown in Fig. 5, and in the base down orientation in Fig. 6. In general it is seen that: (i) as the Reynolds number decreases below $\text{Re}\approx 100$ the drag coefficients approach that of a sphere; and (ii) the drag coefficients reach minima somewhere between $300\lesssim\text{Re}\lesssim 1000$ and increase again as the Reynolds number increases beyond $\text{Re}\gtrsim 1000$. The steady increase of the Best number with increasing Reynolds number indicates that larger

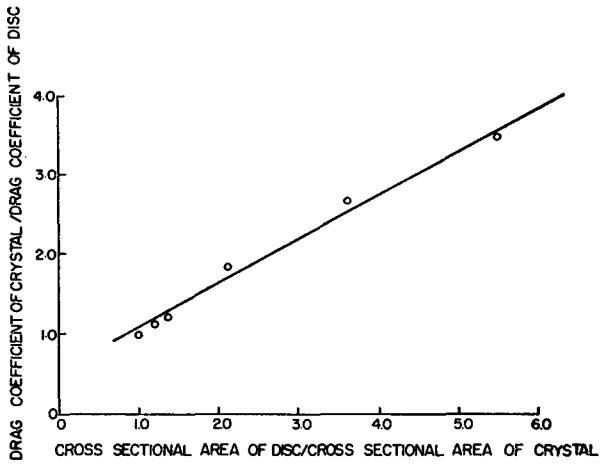

FIG. 4. The ratio of the drag coefficients for the six model crystals to that for the disc as a function of ratio of the corresponding cross-sectional areas.

particles always fall faster than smaller ones of the same shape.

The region where the drag coefficient decreases as the Reynolds number increases is associated with relatively stable fall. A reversal of this trend is caused by oscillations which increase the drag and cause the detailed features of the drag coefficient curves.

The non-translatory motions of the conical models can be split up into two types of roughly periodic oscilla-

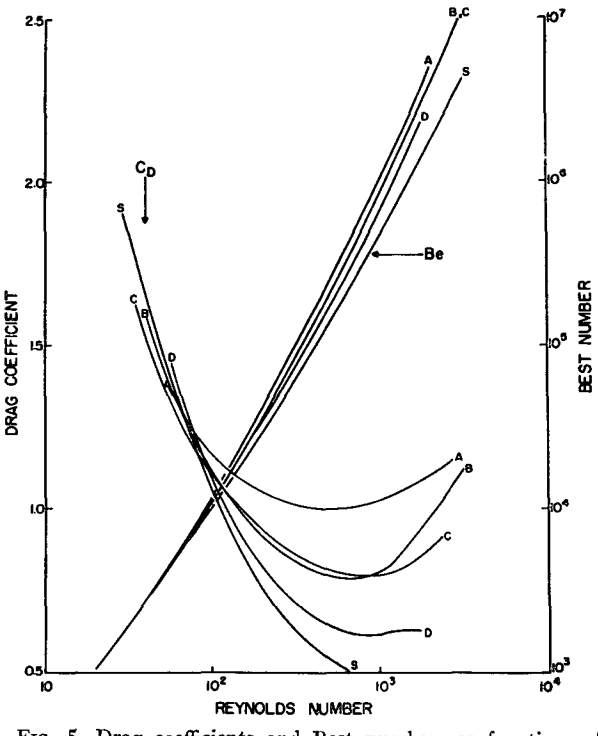

FIG. 5. Drag coefficients and Best numbers as functions of Reynolds number for the conical models released *apex down:* A 90° cone-spherical sector, B 70° cone-spherical sector, C 90° cone-hemisphere, D 90° teardrop, S sphere.

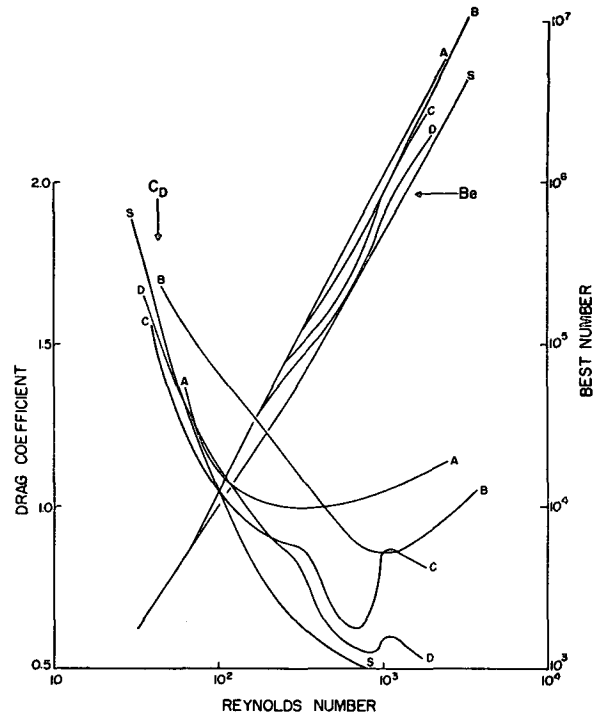

FIG. 6. Same as Fig. 5 except for conical models released *base down.*

tions. The first is a sideways oscillation of the center of mass with a frequency $\leqslant 0.2$ Hz and amplitudes up to 1–2 particle diameters, depending on the model and Reynolds number. The second type is an angular oscillation or swinging of the axis of rotational symmetry with a frequency from 0.1–1 Hz.

The motions of the four conical models are summarized in Fig. 7. They were arbitrarily divided into five ranges of oscillations of the axis from stable to

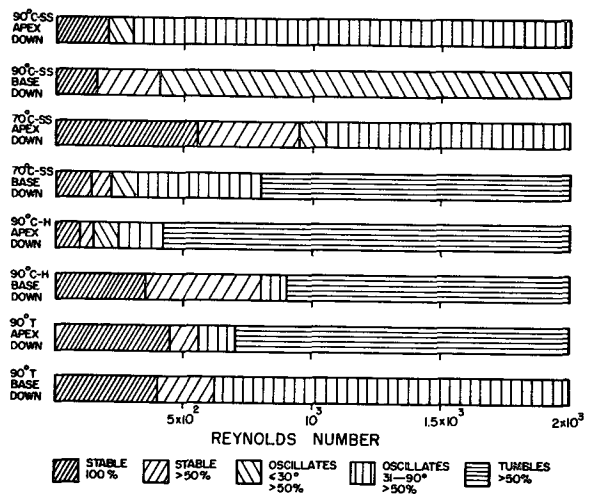

FIG. 7. Degree of oscillation of conical models as a function of Reynolds number: C-SS cone-spherical sector, C-H cone-hemisphere, T teardrop.

tumbling, with the boundaries between ranges accurate to about ±10% of the Reynolds number. From five to ten tests were made at a given Reynolds number, the type of hatching indicating the most frequent degree of oscillation observed. It should be noted that the 90° teardrop shaped model is falling stably in a sideways position, independent of the position of release. Nevertheless, tumbling is reported at higher Reynolds numbers when released in the apex down position, because the teardrop model carries out one or more complete rotations to reach that stable sideways position. This peculiar alignment of the particle axis could explain why an ellipsoidal hailstone often contains a conical embryo particle with its main axis oriented at a right angle to the hailstone's stable fall direction, a direction parallel to its smallest axis.

The 90° cone-spherical sector is more stable falling in the base down orientation, while the 70° cone-spherical sector is more stable falling in the apex down orientation. The latter represents the most stable combination of model and position for Re < 1000. The former combination, however, never shows oscillations >30° with an occurrence of more than 50%, even at Re > 1000. The 90° cone-hemisphere is more stable falling in the base down orientation.

A discussion of the origin of the oscillations cannot be carried out here, as these secondary motions will be connected with the still unknown shedding of vortices in the wakes of the models or special boundary effects. In addition, it has to be pointed out that the stability situation for atmospheric particles may also be affected by a nonhomogeneous density distribution within single hydrometeors.

Maximum possible errors in the drag coefficients are ±10% for the conical and ±5% for the snow crystal models, and in the Reynolds numbers ±5% for the conical and ±3% for the snow crystal models. Maximum possible errors in the Best numbers are ±20% for the conical and ±11% for the snow crystal models. These could be reduced by a factor of 2 if the Best numbers were calculated directly from the properties of particles and air. However, the increase in accuracy would not be apparent in the log-log plot used to present the data.

4. Calculation of terminal velocities in the atmosphere

A sample calculation of the terminal velocities of particles corresponding to the models is performed for the 500-mb level of a typical Colorado hailcloud (Beckwith, 1960). The snow crystals, the small hail particles and a sphere (for comparison) were assumed to have ice density, whereas a typical density of 0.6 gm cm^{-3} was used for graupel. The calculated fall velocities for given sizes (Table 2) demonstrate the considerable variation as a function of shape; dendrites, for example, fall with half the velocity of discs of roughly four times their weight. Similar calculations can be performed for any level in the atmosphere and any particle size by making use of the Reynolds number vs Best number relationships presented earlier (Figs. 3 and 5).

5. Summary and conclusions

Drag coefficients and Best numbers for models of planar snow crystals, conical graupel and small hail have been calculated from experimental data as a function of Reynolds number. On this basis, terminal velocities of similarly shaped particles falling in the atmosphere can be calculated.

The drag coefficient curves for the snow crystal models were found to be approximately parallel to the one for the disc. The latter shape has the lowest drag coefficient at any given Reynolds number. It was found that drag coefficients of planar crystals are linearly

TABLE 2. Calculated terminal velocities, Best numbers and Reynolds numbers of test particles at 500 mb. Parameters used in the calculation are: altitude 4307 m, temperature −12.3C, viscosity of air 1.65×10^{-2} cP, and density of air 6.66×10^{-4} gm cm^{-3}. Conical particles are assumed to fall with the apex downward. The thickness of the particles is h, their total height H.

Particle type	D (cm)	h (cm)	Volume (cm^3)	Density ρ (gm cm^{-3})	Best number Be	Reynolds number Re	Terminal velocity V (cm sec^{-1})
Disc	0.1	0.002	1.57×10^{-5}	0.195	877	17.8	44.1
Hexagonal plate	0.1	0.002	1.31×10^{-5}	0.915	877	15.8	39.1
Broad-branched	0.1	0.002	1.16×10^{-5}	0.915	877	14.8	36.6
Stellar with plate	0.1	0.002	0.74×10^{-5}	0.915	877	11.4	28.2
Dendrite	0.1	0.002	0.44×10^{-5}	0.915	877	8.7	21.5
Stellar	0.1	0.002	0.29×10^{-5}	0.915	877	7.0	17.3
		H (cm)					
90° cone-spherical segment	0.2	0.142	1.75×10^{-3}	0.6	6.44×10^{4}	250	310
70° cone-spherical segment	0.2	0.172	2.30×10^{-3}	0.6	7.48×10^{4}	300	372
sphere	0.2	0.2	4.19×10^{-3}	0.6	1.54×10^{5}	540	668
90° cone-hemisphere	0.2	0.194	3.01×10^{-3}	0.915	1.69×10^{5}	440	546
90° teardrop	0.2	0.232	5.00×10^{-3}	0.915	2.82×10^{5}	700	868
sphere	0.2	0.2	4.19×10^{-3}	0.915	2.36×10^{5}	700	868

related to those of discs if the ratio of the cross-sectional areas is used as a parameter.

The drag coefficient curves for the conical graupel and small hail models have a minimum between Reynolds numbers of about 300 and 1000. Drag coefficients in this region range from 0.6–1.1 depending on model and orientation. The curves approach that of a sphere for $Re \leqslant 10^2$. At Re values beyond the minimum the drag is increasing due to oscillations.

Oscillations are not existent or not important for snow crystals and for small conical particles. However, as soon as graupel and small hail reach sizes corresponding to Reynolds numbers of about 200–800, then secondary motions start to affect the fall and increase the drag coefficients. An investigation of the stability of the position of conical particles gave the Reynolds number ranges for stable free fall, oscillations of two different degrees, and tumbling.

A natural sequence of growth by accretion from a dendritic snow crystal to a graupel, then a small hail particle and finally to a hailstone [as observed by List (1958)] can easily be followed by Fig. 3. A dendritic crystal falling in a cloud of supercooled water droplets catches them and becomes filled in, while the total thickness increases. The drag coefficient drops to the disc-like equivalent. Further accretion of cloud droplets will cause the conglomerate to grow in the direction of the vertical axis (Arenberg, 1941), and a transition is made to the graupel stage with the drag coefficients behaving accordingly. As the particle continues to grow by accretion, it falls faster, the heat transfer is less effective, and the accreted water partially enters the ice framework of the graupel, causing a densification. This is the small hail stage where tumbling may start; the drag coefficient changes accordingly and eventually the particle falls as a roughly spherical hailstone, represented by the lowest curve in Fig. 3.

Acknowledgments. This study was carried out within a research program sponsored by the National Research Council of Canada. One of the authors (R. S. S.) is indebted to the Meteorological Service of Canada for financial support and to the University of Toronto for an E. F. Burton Fellowship.

REFERENCES

Arenberg, D. L., 1941: The formation of small hail and snow pellets. *Bull. Amer. Meteor. Soc.*, **22**, 113–116.

Beckwith, W. B., 1960: Analysis of hailstorms in the Denver network, 1949–1958. *Physics of Precipitation*, Geophys. Monogr. No. 5, Amer. Geophys. Union, 345–353.

Best, A. C., 1950: Empirical formulae for the terminal velocity of water drops falling through the atmosphere. *Quart. J. Roy. Meteor. Soc.*, **76**, 302–311.

Goldburg, A., and B. H. Florsheim, 1966: Transition and Strouhal number for the incompressible wake of various bodies. *Phys. Fluids*, **9**, 45–50.

Jayaweera, K. O. L. F., and B. J. Mason, 1965: The behavior of freely falling cylinders and cones in a viscous liquid. *J. Fluid Mech.*, **22**, 709–720.

——, and R. E. Cottis, 1969: Fall velocities of plate-like and columnar-ice crystals. *Quart. J. Roy. Meteor. Soc.*, **95**, 703–709.

List, R., 1958: Kennzeichen atmosphärischer Eispartikeln, Part 1. *Z. Angew. Math. Phys.*, **9a**, 180–192.

——, 1959: Zur Aerodynamik von Hagelkörnern. *Z. Angew. Math. Phys.*, **10**, 143–159.

——, 1966: On the simulation of physical processes occurring in clouds. *Bull. Amer. Meteor. Soc.*, **47**, 393–396.

Nagel, J. F., 1962: On the shape of graupel and hailstones. *Weather Bureau Notes, South Africa*, **11**, 77–88.

Nakaya, U., and Terada, 1934: Simultaneous observations of the mass, falling velocity and form of individual snow crystals. *J. Fac. Sci. Hokkaido Univ.*, Ser. 2, **1**, 191–200.

Podzimek, J., 1965: Movement of ice particles in the atmosphere. *Proc. Intern. Conf. Cloud Physics*, Tokyo and Sapporo, 224–230.

——, 1968: Aerodynamic conditions for ice crystal aggregation. *Proc. Intern. Conf. Cloud Physics*, Toronto, 295–299.

Wieselsberger, C., 1922: Weitere Feststellungen über die Gesetze des Flüssigkeits u. Luftwiderstandes. *Phys. Z.*, **23**, 219–224.

Willmarth, W. W., N. E. Hawk and R. L. Harvey, 1964: Steady and unsteady motions and wakes of freely falling discs. *Phys. Fluids*, **7**, 197–208.